

Wireless Sensor Networks Based on the Generalized Approach to Signal Processing with Fading Channels and Receive Antenna Array

VYACHESLAV TUZLUKOV, WON-SIK YOON, YONG DEAK KIM

Department of Electrical and Computer Engineering

College of Information Technology, Ajou University

San 5, Wonchon-dong, Paldal-gu, Suwon 442-749

KOREA, REPUBLIC OF

Email: tuzlukov@ajou.ac.kr, wsyoon@ajou.ac.kr, yongdkim@ajou.ac.kr

Abstract: -We consider M -ary wireless sensor network based on the generalized approach to signal processing in the presence of noise [1–5] with K sensor nodes over a space diversity channel, consisting of a single transmit antenna for each sensor node and multiple receive antennas. We examine the phase coherent wavefront fading model. In the case of wavefront fading, the fade is constant across the face of the receive antenna and we can associate an angle of arrival to the signal. We present a variation of the multiple-signal classification (MUSIC) algorithm [6] for estimating this parameter and use it to form a spatial beam. We develop the detection strategy based on the generalized approach to signal processing in noise. We then consider blind extensions of the generalized detector based on subspace tracking, which do not require a prior model for the interfering sensor node's signals

Key-Words: - Antenna arrays, blind detection, direction of arrival (DOA) estimation, fading channels, multiuser detection, space-time processing, generalized detector.

1 Introduction

M -ary modulation schemes are commonly employed on noncoherent channels in wireless sensor networks. For example, Walsh codes are used on uplink of the channel, which are decoded noncoherently. This is just one example of orthogonal multipulse modulation, and noncoherent frequency-shift keying is another. Other common techniques employ differential phase encoding and then perform detection by processing the received data two symbols at a time. The effective model employed in such detection is of an M^2 -ary constellation with each two-dimensional transmit vector corresponding to the present and previous information bit [7].

In this paper, we consider several extensions of the noncoherent multiuser detection results of [4,8–10] for M -ary wireless sensor networks to the multiple-antenna fading channel. We consider the basic model: the fading process for each sensor node is assumed constant across the face of the array. This is called coherent wavefront fading.

It is assumed that the fading coefficients remain constant over the duration of each symbol. They are, however, allowed to vary arbitrarily (even independently) from symbol to symbol. Such a block fading model is applicable to rapidly fading channels and/or to frequency-hopping and block-interleaved wireless

sensor network systems. The multiuser wireless sensor network channel is further assumed to be synchronous, but this assumption may be relaxed when the blind generalized detector is employed.

For the coherent wavefront fading channel considered in this paper, we are able to associate a direction of arrival (DOA) with each sensor node and employ a detection rule based on the generalized approach to signal processing in the presence of noise, which exploit this structure. The detection scheme is extension of the generalized detector presented in [1–5], the main difference being the inclusion of the DOA. We use a technique for estimating the DOA discussed in [11] which is inspired by the multiple-signal classification (MUSIC) algorithm [6].

The performance of the generalized detector is analyzed through the use of a union upper bound on the symbol error probability, drawing in part on the asymptotic analysis techniques of [12] together with some geometrical insights. It is shown that the performance of the generalized detector achieves the expected dependency on the signal-to-noise ratio (SNR). In other words, falls of like $(1/\text{SNR})$ for the wavefront fading channel so long as there is some separation between the signal subspace and the interference subspaces of the other sensor nodes. Finally, a blind version of the generalized detector is specified.

2 Antenna Array Model

Our convention will be that K sensor nodes, each communicating from an M -ary signal set and a single-antenna transmitter, are communicating with an L -element receiver. The orthonormal basis for the KM signaling waveforms has cardinality $N \leq KM$. At the ℓ -th antenna element we receive the continuous-time signal

$$x_\ell(t) = \sum_{k=1}^K \alpha_\ell(k) a_{m_k}(t) + n_\ell(t), \quad (1)$$

where $a_{m_k}(t)$ is the signal transmitted by sensor node k from a set of cardinality M , $\alpha_\ell(k)$ is the fading coefficient for the path connecting sensor node k to the ℓ -th antenna, and $n_\ell(t)$ is circularly symmetric complex Gaussian noise.

By matching to an N -dimensional orthonormal basis, $\{u_n(t)\}_1^N$, for the joint signal space spanned by all of the signals, $\{a_{m_k}(t)\}$, we obtain the measurement $\mathbf{y}_\ell \in \mathfrak{R}^N$

$$\begin{aligned} \mathbf{y}_\ell &= \sum_{k=1}^K \alpha_\ell(k) \mathbf{g}_{m_k}(k) + \mathbf{n}_\ell \\ &= \sum_{k=1}^K \alpha_\ell(k) \mathbf{G}(k) \mathbf{b}(k) + \mathbf{n}_\ell. \end{aligned} \quad (2)$$

Here, $\mathbf{g}_{m_k}(k)$ is a vector containing the expansion coefficients for the k -th sensor node's m_k -th signal

$$\{\mathbf{g}_{m_k}(k)\}_n = \int a_{m_k}(t) u_n^*(t) dt. \quad (3)$$

The matrix $[\mathbf{G}(1), \mathbf{G}(2), \dots, \mathbf{G}(K)]$ contains the signal vectors for each sensor node with

$$\mathbf{G}(k) = [\mathbf{g}_1(k), \mathbf{g}_2(k), \dots, \mathbf{g}_M(k)]. \quad (4)$$

The vector $[\mathbf{b}^T(1), \mathbf{b}^T(2), \dots, \mathbf{b}^T(K)]^T$, and $MK \times 1$ vector with each $\mathbf{b}(k)$, a column of the $M \times M$ identity matrix, selects the signal transmitted by sensor node k . That is,

$$\mathbf{G}(k) \mathbf{b}_m(k) = \mathbf{g}_{m_k}(k). \quad (5)$$

The additive noise, $\mathbf{n}_\ell \in \mathfrak{R}^N$, is a circularly symmetric white Gaussian vector with correlation

$$M[\mathbf{n}_\ell \mathbf{n}_\ell^*] = \sigma^2 \mathbf{I}_N. \quad (6)$$

If we are interested in sensor node k , we may rewrite our model with respect to this sensor node as

$$\mathbf{y}_\ell = \alpha_\ell \mathbf{g}_m + \mathbf{S} \boldsymbol{\rho}_\ell + \mathbf{n}_\ell, \quad (7)$$

where we have dropped the dependency on k and have collected all of the multiple-access interference (MAI) into the vector

$$\mathbf{S} \boldsymbol{\rho}_\ell = \sum_{k \neq k'}^K \alpha_\ell(k') \mathbf{g}_{m_{k'}}(k'). \quad (8)$$

Thus, the matrix \mathbf{S} contains all $M(K-1)$ interfering signal vectors, and the vector $\boldsymbol{\rho}_\ell \in \mathfrak{R}^{M(K-1)}$ is formed by stacking the vectors $\alpha_\ell(k') \mathbf{b}(k')$ for $k \neq k'$.

We may now collect the measurements into the $LN \times 1$ vector

$$\mathbf{y} = [\mathbf{y}_1^T, \mathbf{y}_2^T, \dots, \mathbf{y}_L^T]^T \in \mathfrak{R}^{LN}, \quad (9)$$

i.e.,

$$\begin{aligned} \mathbf{y} &= \sum_{k=1}^K [\mathbf{I}_L \otimes \mathbf{G}(k)] \cdot [\alpha(k) \otimes \mathbf{b}(k)] + \mathbf{n} \\ &= \mathcal{F} \mathbf{c} + \mathbf{n}, \end{aligned} \quad (10)$$

where

$$\mathcal{F} = [\mathbf{I}_L \otimes \mathbf{G}(1) \cdots \mathbf{I}_L \otimes \mathbf{G}(K)] \quad (11)$$

contains all of the sensor node's KLM space-time signaling vectors,

$$\alpha(k) = [\alpha_1(k) \cdots \alpha_L(k)]^T, \quad (12)$$

and

$$\mathbf{c} = \begin{bmatrix} \alpha(1) \otimes \mathbf{b}(1) \\ \vdots \\ \alpha(K) \otimes \mathbf{b}(K) \end{bmatrix}. \quad (13)$$

The symbol \otimes denotes the Kronecker product of two matrices [13].

We can rewrite this model with respect to a particular sensor node as

$$\begin{aligned} \mathbf{y} &= [\mathbf{I}_L \otimes \mathbf{g}_m] \boldsymbol{\alpha} + [\mathbf{I}_L \otimes \mathbf{S}] \boldsymbol{\rho} + \mathbf{n} \\ &= \mathcal{H}_m \boldsymbol{\alpha} + \mathcal{S} \boldsymbol{\rho} + \mathbf{n}, \end{aligned} \quad (14)$$

where

$$\begin{cases} \mathcal{H}_m = \mathbf{I}_L \otimes \mathbf{g}_m, \\ \mathcal{S} = \mathbf{I}_L \otimes \mathbf{S}, \\ \boldsymbol{\rho} = [\boldsymbol{\rho}_1^T, \dots, \boldsymbol{\rho}_1^T]^T \in \mathfrak{R}^{LM(K-1)}, \end{cases} \quad (15)$$

and we have dropped the explicit dependence of these parameters on k .

We note that the measurement space has dimension LN , whereas the signal and interference lie in subspaces of respective dimensions L and $L(K-1)$.

We see that low space dimension L can be compensated for by a large time (or spreading) dimension N , or vice versa, for separating signal and interference, provided these degrees of freedom are exploited with an appropriate signal design.

3 Coherent Fading Channel Model

Consider the case of phase-coherent fading, meaning that the fading parameters for each sensor node are

modeled as

$$\alpha_\ell(k) = \alpha(k)s_\ell(\theta_k), \quad (16)$$

where $\alpha(k)$ is a constant complex fading parameter across the array, θ_k is the DOA of the k -th sensor node's signal relative to the array geometry, and $s_\ell(\theta_k)$ is the response of the ℓ -th antenna sensor to a narrowband signal arriving from θ_k . The similar model was discussed in more detail in [13].

In this case, the model of (5) simplifies to

$$\mathbf{y} = \sum_{k=1}^K \alpha(k) [\mathbf{I}_L \otimes \mathbf{g}_{m_k}(k)] \cdot \mathbf{s}(\theta_k) + \mathbf{n}, \quad (17)$$

where

$$\mathbf{s}(\theta_k) = [s_1(\theta_k), \dots, s_L(\theta_k)]^T \quad (18)$$

is a steering vector in direction θ_k . If the DOA for each of the sensor nodes is known, we may simplify our model with respect to sensor node k as

$$\mathbf{y} = \alpha \mathbf{h}_m + \mathbf{R} \boldsymbol{\beta} + \mathbf{n}, \quad (19)$$

where $\mathbf{h}_m(k)$ is the following signal vector, defined by its signal matrix $\mathcal{H}_m(k)$ and arrival angle θ_k

$$\mathbf{h}_m(k) = [\mathbf{I}_L \otimes \mathbf{g}_m(k)] \cdot \mathbf{s}(\theta_k) = \mathcal{H}_m(k) \cdot \mathbf{s}(\theta_k). \quad (20)$$

\mathbf{R} is the matrix containing the $(K-1)M$ interference vectors $\{\mathbf{h}_{m_{k'}}(k')\}$ for $k' \neq k$, and $\boldsymbol{\beta}$ is formed by stacking the vectors $\alpha(k')\mathbf{h}_{m_{k'}}(k')$ for $k' \neq k$, i.e.,

$$\mathbf{R} \boldsymbol{\beta} = \sum_{k' \neq k}^K \alpha(k') \mathbf{h}_{m_{k'}}(k'). \quad (21)$$

Notice that $\{\mathbf{h}_m(k)\}$, the DOA-resolved signals should not be confused with $\{\mathbf{g}_m(k)\}$, the original, unresolved signals.

Except for the important details about the space-time structure of \mathbf{h}_m and \mathbf{R} , our model is now algebraically identical to that considered in [1–5], and the generalized detector contained there may be used on this channel without essential modification. The interference matrix, \mathbf{R} , is the space-time (or, more accurately, the space-dimension) matrix formed by the vectors $[\mathbf{I}_L \otimes \mathbf{g}_{m_{k'}}(k')] \cdot \mathbf{s}(\theta_{k'})$ for $k' \neq k$. If we choose the basis functions to be time-delayed versions of a common pulse shape, as in direct-sequence code-division multiple access (DS-CDMA) or time-division multiple access (TDMA) wireless sensor networks, we can consider \mathbf{R} to be the space-time interference matrix. In general, the basis functions need not have such an interpretation. They could be chosen to efficiently manage bandwidth, for example.

4 Generalized Detector

The space-time generalized detector (GD) is discussed in more detail in [5]. In the case at hand, the decision-making rule is defined by maximizing the likelihood functions

$$f_m(\mathbf{y}) = \frac{1}{(\pi\sigma^2)^{LN}} \exp \left\{ \frac{1}{\sigma^2} \|\mathbf{y} - \mathbf{h}_m \alpha - \mathbf{R} \boldsymbol{\beta}\|^2 \right\} \quad (22)$$

over the unknown parameters α and $\boldsymbol{\beta}$. The result is

$$\begin{aligned} \hat{m}_{GD} &= \arg \max_m \frac{|2\mathbf{h}_m \mathbf{P}_{\mathbf{R}}^\perp \mathbf{y}^* - \mathbf{y}^* \mathbf{P}_{\mathbf{R}}^\perp \mathbf{y} + \mathbf{n}_1^* \mathbf{P}_{\mathbf{R}}^\perp \mathbf{n}_1|^2}{\|\mathbf{P}_{\mathbf{R}}^\perp \mathbf{h}_m\|^2} \\ &= \arg \max_m [2\mathbf{h}_m \mathbf{P}_{\mathbf{P}_{\mathbf{R}}^\perp \mathbf{h}_m} \mathbf{y}^* - \mathbf{y}^* \mathbf{P}_{\mathbf{P}_{\mathbf{R}}^\perp \mathbf{h}_m} \mathbf{y} + \mathbf{n}_1^* \mathbf{P}_{\mathbf{P}_{\mathbf{R}}^\perp \mathbf{h}_m} \mathbf{n}_1], \end{aligned} \quad (23)$$

where \mathbf{n}_1 is a vector of an additional noise source according to the generalized approach to signal processing in the presence of noise [1–5]. The right most form of (23) shows that the GD to be a matched subspace detector [14], using the projection onto the one-dimensional subspace spanned by the vector $\mathbf{P}_{\mathbf{R}}^\perp \mathbf{h}_m$. The $N \times N$ projection operator onto this subspace is denoted by $\mathbf{P}_{\mathbf{P}_{\mathbf{R}}^\perp \mathbf{h}_m}$.

The GD detector chooses the signal, \mathbf{h}_m , which has the greatest direction cosine with the measurement in the subspace orthogonal to the interference, $\langle \mathbf{R} \rangle^\perp$. This detector is invariant to complex scaling of the data and to translations of the data in the interference subspace, $\langle \mathbf{R} \rangle$. A more thorough discussion of the geometry and invariances of the GD detector is presented in [5].

The GD detector for wavefront fading bears comment, for it reveals an important decomposition of the space-time receiver. To make this point, let us rewrite the quadratic form in (23) as

$$\begin{aligned} &\arg \max_m [2\mathbf{h}_m \mathbf{P}_{\mathbf{P}_{\mathbf{R}}^\perp \mathbf{h}_m} \mathbf{y}^* - \mathbf{y}^* \mathbf{P}_{\mathbf{P}_{\mathbf{R}}^\perp \mathbf{h}_m} \mathbf{y} + \mathbf{n}_1^* \mathbf{P}_{\mathbf{P}_{\mathbf{R}}^\perp \mathbf{h}_m} \mathbf{n}_1] = \\ &\arg \max_m \left\{ \frac{2s^*(\theta_k) [\mathbf{I}_L \otimes \mathbf{g}_m]^* \mathbf{P}_{\mathbf{R}}^\perp \mathbf{y}}{s^*(\theta_k) [\mathbf{I}_L \otimes \mathbf{g}_m]^* \mathbf{P}_{\mathbf{R}}^\perp [\mathbf{I}_L \otimes \mathbf{g}_m] \mathbf{s}(\theta_k)} \right. \\ &\quad - \frac{\mathbf{y}^* \mathbf{P}_{\mathbf{R}}^\perp \mathbf{y}}{s^*(\theta_k) [\mathbf{I}_L \otimes \mathbf{g}_m]^* \mathbf{P}_{\mathbf{R}}^\perp [\mathbf{I}_L \otimes \mathbf{g}_m] \mathbf{s}(\theta_k)} \\ &\quad \left. + \frac{\mathbf{n}_1^* \mathbf{P}_{\mathbf{R}}^\perp \mathbf{n}_1}{s^*(\theta_k) [\mathbf{I}_L \otimes \mathbf{g}_m]^* \mathbf{P}_{\mathbf{R}}^\perp [\mathbf{I}_L \otimes \mathbf{g}_m] \mathbf{s}(\theta_k)} \right\}. \end{aligned} \quad (24)$$

Thus, the GD consists of a space-time interference rejection operator $\mathbf{P}_{\mathbf{R}}^\perp$, followed by temporal matched filtering and then spatial matched filtering (beam-

forming). There is no approximation in this factored implementation of the space-time GD for M -ary wireless sensor networks over the wavefront fading channel.

5 Performance of the GD

The performance of the GD has been analyzed on the noncoherent additive white Gaussian noise channel in [15]. In this section, we will extend this analysis to the Rayleigh fading channel. We will employ the union bound on the probability of error

$$P_{er} \leq \frac{1}{M} \sum_{m=1}^M \sum_{\ell=1, \ell \neq m}^M P(m, \ell), \quad (25)$$

where $P(m, \ell)$ is the probability that the ℓ -th decision statistic is greater than the m -th statistic when signal m is transmitted. We derive asymptotic (in the SNR) expressions for these bounds, so we will only consider zero-forcing GD detector. We will need expressions for the two-signal error probability for the GD.

The pairwise probability of error is $P_{GD}(m, \ell)$

$$= \text{Prob} \left\{ \frac{|2\mathbf{h}_m \mathbf{P}_R^\perp \mathbf{y}^* - \mathbf{y}^* \mathbf{P}_R^\perp \mathbf{y} + \mathbf{n}_1^* \mathbf{P}_R^\perp \mathbf{n}_1|^2}{\|\mathbf{P}_R^\perp \mathbf{h}_m\|^2} < \frac{|2\mathbf{h}_\ell \mathbf{P}_R^\perp \mathbf{y}^* - \mathbf{y}^* \mathbf{P}_R^\perp \mathbf{y} + \mathbf{n}_1^* \mathbf{P}_R^\perp \mathbf{n}_1|^2}{\|\mathbf{P}_R^\perp \mathbf{h}_\ell\|^2} \right\} \quad (26)$$

if signal \mathbf{h}_m was transmitted. Letting

$$\begin{cases} \mathbf{P}_m = \mathbf{P}_{\mathbf{P}_R^\perp \mathbf{h}_m}; \\ \mathbf{P}_\ell = \mathbf{P}_{\mathbf{P}_R^\perp \mathbf{h}_\ell}; \\ \Delta \mathbf{P}_{m,\ell} = \mathbf{P}_m - \mathbf{P}_\ell, \end{cases} \quad (27)$$

we have

$$P_{GD}(m, \ell) = \text{Prob} \{ \mathbf{y}^* \Delta \mathbf{P}_{m,\ell} \mathbf{y} < 0 \}. \quad (28)$$

Using the results of [16], we find the characteristic function of the quadratic form

$$z = \mathbf{y}^* \Delta \mathbf{P}_{m,\ell} \mathbf{y} \quad (29)$$

to be

$$\Theta_z(r) = \frac{1}{\|2\mathbf{I} + r(\mu^2 \mathbf{P}_R^\perp \mathbf{h}_m \mathbf{h}_m^* \mathbf{P}_R^\perp + 4\sigma^4 \mathbf{I}) \Delta \mathbf{P}_{m,\ell}\|}, \quad (30)$$

where $\|\dots\|$ is a determinant,

$$\mu^2 = M[|\alpha(k)|^2] \quad (31)$$

is the variance of the wavefront fade for sensor node k .

To determine the probability of error, we need to find the two nonzero eigenvalues, λ_{GD} , of the rank-two matrix

$$(\mu^2 \mathbf{P}_R^\perp \mathbf{h}_m \mathbf{h}_m^* \mathbf{P}_R^\perp + 4\sigma^4 \mathbf{I}) \Delta \mathbf{P}_{m,\ell}. \quad (32)$$

These two eigenvalues are found via the quadratic equation to be

$$\begin{aligned} \lambda_{1,2}^{GD} = & 0.5 E_m \mu^2 \chi_{m,\ell} \\ & \pm 0.5 \sqrt{E_m^2 \mu^4 \chi_{m,\ell}^2 + 16 \chi_{m,\ell} \sigma^4 (E_m \mu^2 + 4\sigma^4)}, \end{aligned} \quad (33)$$

where

$$\begin{aligned} \chi_{m,\ell} = & 1 - \frac{|\mathbf{h}_m^* \mathbf{P}_R^\perp \mathbf{h}_\ell|^2}{\|\mathbf{P}_R^\perp \mathbf{h}_m\|^2 \|\mathbf{P}_R^\perp \mathbf{h}_\ell\|^2} \\ = & \sin^2[\mathbf{P}_R^\perp \mathbf{h}_m, \mathbf{P}_R^\perp \mathbf{h}_\ell] \end{aligned} \quad (34)$$

is the sine squared of the angle between $\mathbf{P}_R^\perp \mathbf{h}_m$ and $\mathbf{P}_R^\perp \mathbf{h}_\ell$;

$$E_m = \mathbf{h}_m^* \mathbf{P}_R^\perp \mathbf{h}_m = \|\mathbf{h}_m\|^2 \cdot \sin^2[\mathbf{h}_m, \mathbf{R}] \quad (35)$$

is the sine squared of the principal angle between the vector \mathbf{h}_m and the subspace $\langle \mathbf{R} \rangle$ weighted by the signal energy. The corresponding error probability is then

$$P_{GD}(m, \ell) = \frac{1}{1 - \frac{\lambda_1^{GD}}{\lambda_2^{GD}}}, \quad (36)$$

where we have identified λ_2^{GD} as the positive root appearing in (33).

By expanding the square root term in a Taylor series about $4\sigma^4$, we find that asymptotically (in the SNR) the eigenvalues are given by

$$\begin{cases} \lambda_1^{GD} \cong -4\sigma^4, \\ \lambda_2^{GD} \cong E_m \mu^2 \chi_{m,\ell}. \end{cases} \quad (37)$$

The corresponding asymptotic expression for the pairwise probability of error is

$$P_{GD}(m, \ell) \cong \frac{1}{1 + SNR_{GD}}, \quad (38)$$

where SNR_{GD} is the following SNR:

$$\begin{aligned} SNR_{GD} = & \frac{\mu^2 \|\mathbf{h}_m\|^2}{4\sigma^4} \cdot \sin^2[\mathbf{h}_m, \mathbf{R}] \\ & \times \sin^2[\mathbf{P}_R^\perp \mathbf{h}_m, \mathbf{P}_R^\perp \mathbf{h}_\ell]. \end{aligned} \quad (39)$$

We notice that the probability of error is a function of this effective SNR, which relates the geometry of

the signal set directly to the asymptotic performance of the detector through the sine-squared terms in $\sin^2[\mathbf{P}_R \frac{1}{R} \mathbf{h}_m, \mathbf{P}_R \frac{1}{R} \mathbf{h}_\ell]$ and $\sin^2[\mathbf{h}_m, \mathbf{R}]$.

6 Simulation Results

Now let us consider two examples of multiuser wireless sensor network systems on the wavefront fading channel. In both examples, we have $K=2$ sensor nodes, each employing $M=2$ signals with a processing gain of $N=3$. In each case, a uniform linear array was employed with half wavelength sensor spacing and $L=3$ antenna sensors. For each example, the fading processes for each sensor node were assumed to have the same variance and the sensor nodes employed equal energy signal constellation.

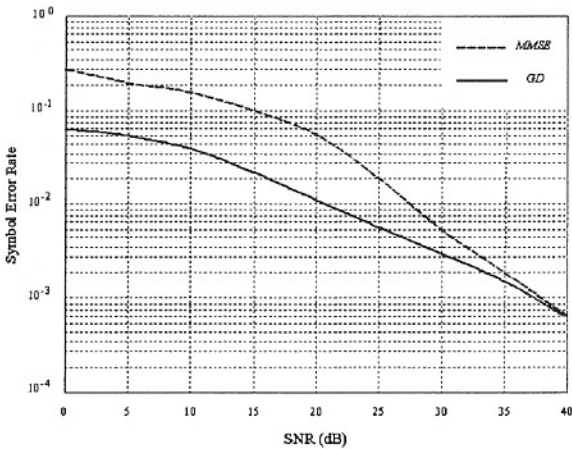


Figure 1. Symbol error rate versus SNR for the GD and MMSE detector with two sensor nodes.

In the first example, we randomly chose the signals for each sensor node. We fixed the DOAs of the sensor node relative to the receive array to be 0° and 5° for sensor nodes one and two, respectively. In Figure 1, we plot the probability of symbol error for sensor node one as a function of the SNR for the GD and the minimum mean-square error (MMSE) detector for comparison. The GD outperforms the MMSE detector at low SNRs. At high SNRs, the performance of the MMSE detector tends to approach the performance of the GD. Notice that for this example, the error bounds derived in (38) agree quite well with the experimental data.

The next example we consider is the case of identical waveform signaling, meaning that the two sensor nodes employ exactly the same signals, i.e., $\mathbf{G}(1) = \mathbf{G}(2)$. For this case, all of the interference rejection comes from beamforming. This is sometimes called angle-division multiple access (ADMA). Notice that bandwidth can be easily managed in this scheme as each sensor node employs exactly the same frequency band; sensor nodes can be added without increasing the bandwidth so long as there are enough sensors in the array to resolve the sensor nodes' DOAs. Since the signal separation between the two sensor nodes is now only a function of their arrival angles, we fixed sensor node one's DOA to 50° and varied the interfering sensor node's DOA from -90° to 90° . The SNR was fixed at 20 dB. The results of this experiment are shown in Figure 2, and compared with MMSE detector. We are able to see clearly that the GD outperforms the MMSE detector. We notice that when the interfering sensor node is close to the sensor node user, the performance degradation is severe.

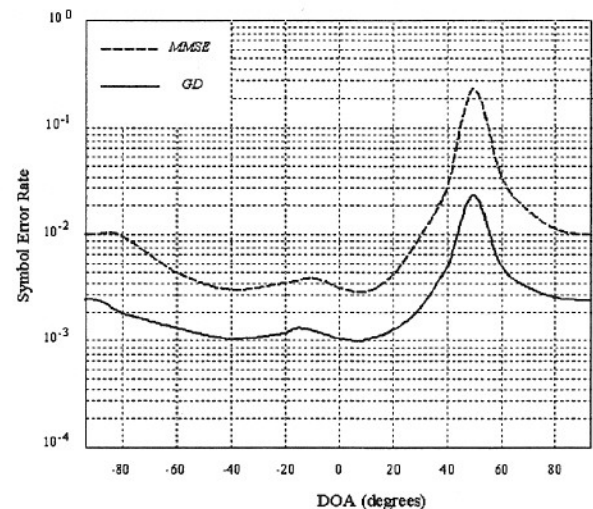


Figure 2. Symbol error rate versus DOA of the interfering sensor node for the GD and MMSE detectors with identical waveform signaling

7 Estimating the DOA

When the DOA of sensor node k is unknown, we must estimate it in order to complete our model for detection. In this section, we propose a modification of the MUSIC algorithm [6] to perform this estimati-

on. In our model for $\mathbf{h}_m(k)$ in (20) we see that the DOA-resolved signal vectors $\{\mathbf{h}_m(k)\}$, all lie in the signal subspace. Let

$$\mathbf{K}_{yy} = M[\mathbf{y}\mathbf{y}^*] \quad (40)$$

have the eigendecomposition

$$\mathbf{K}_{yy} = [\mathbf{U}\mathbf{V}] \cdot \begin{vmatrix} \Lambda_1 + 4\sigma^4\mathbf{I} & 0 \\ 0 & 4\sigma^4\mathbf{I} \end{vmatrix} \cdot \begin{vmatrix} \mathbf{U}^* \\ \mathbf{V}^* \end{vmatrix}, \quad (41)$$

where \mathbf{V} is an orthonormal basis for the orthogonal subspace. Then for each signal vector, $\mathbf{h}_m(k)$, we have

$$\begin{aligned} \mathbf{h}_m^*(k)\mathbf{V}\mathbf{V}^*\mathbf{h}_m(k) &= \mathbf{s}^*(\theta_k) \cdot [\mathbf{I}_L \otimes \mathbf{g}_m(k)]^* \mathbf{V}\mathbf{V}^* \\ &\times [\mathbf{I}_L \otimes \mathbf{g}_m(k)] \cdot \mathbf{s}(\theta_k) = 0. \end{aligned} \quad (42)$$

This suggests that we first estimate $\hat{\mathbf{K}}_{yy}$ and $\hat{\mathbf{V}}$, and then estimate θ_k from the modified MUSIC functional

$$\begin{aligned} \hat{\theta}_k &= \arg \min_{\theta} \left\{ \mathbf{s}^*(\theta) \cdot \left[\sum_{m=1}^M [\mathbf{I}_L \otimes \mathbf{g}_m(k)]^* \hat{\mathbf{V}} \right. \right. \\ &\quad \left. \left. \times \hat{\mathbf{V}}^* [\mathbf{I}_L \otimes \mathbf{g}_m(k)] \right] \cdot \mathbf{s}(\theta) \right\}, \end{aligned} \quad (43)$$

where $\{\mathbf{g}_m(k)\}_1^M$ are the M -ary signals assigned to sensor node k .

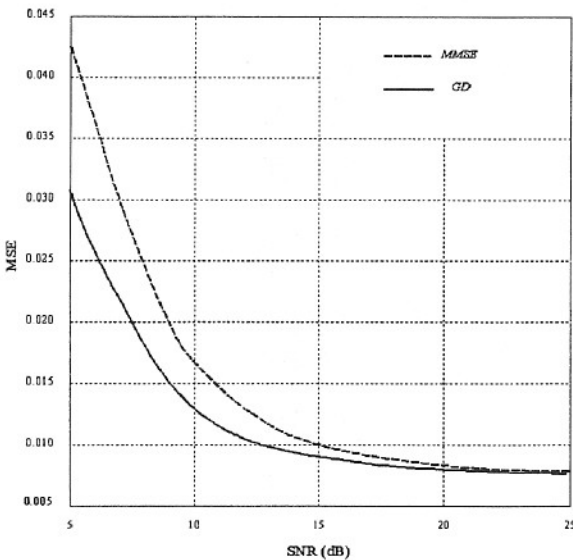


Figure 3. MSE for DOA estimation with the modified MUSIC rule for the GD and MMSE detector.

In Figure 3, we plot the mean squared error (MSE) of our modified MUSIC estimation algorithm for a $K=3$ sensor node channel with $L=2$ receive antennas. The interfering sensor nodes have energy levels 7 dB above the desired sensor node and all sensor nodes employed an $M=3$ signal set with dimension $N=12$. The signal set for each sensor node was chosen randomly. In addition, we can compare the GD and MMSE detectors and see the GD possesses the lower MSE relative to the MMSE detector.

A key observation is that this technique is blind with respect to the interfering sensor nodes. This means that it can be used to estimate the DOA of each sensor node independently. It can also be incorporated into blind detectors of the type discussed in [4,5].

8 Conclusions

For wavefront fading, we may associate a DOA, θ_k , to each sensor node and exploit this structure to form a one-dimensional matched subspace GD, which performs spatial beamforming and temporal matched filtering separately. Comparative analysis between the proposed GD and MMSE detector shows a superiority of the first detector. With these results, we can analyze the important special case of wavefront fading channel. The extension of these results will include multiple transmit antennas.

Acknowledgment:

This work was supported in part by participation within the limits of the project "A Study on Wireless Sensor Networks for Medical Information" sponsored by IITA, Korea.

References:

- [1] V. Tuzlukov, *Signal Processing in Noise: A New Methodology*, IEC, Minsk, 1998.
- [2] V. Tuzlukov, "A new approach to signal detection", *Digital Signal Processing: A Review Journal*, Vol. 8, No. 3, 1998, pp. 166–184.
- [3] V. Tuzlukov, *Signal Detection Theory*, Springer-Verlag, New York, 2001.
- [4] V. Tuzlukov, *Signal Processing Noise*, CRC Press, Boca Raton, London, New York, Washington DC, 2002.
- [5] V. Tuzlukov, *Signal and Image Processing in Navigational Systems*, CRC Press, Boca Raton, London, New York, Washington DC, 2004.

- [6] R. Schmidt, "A signal subspace approach to multiple emitter location and spectral estimation," *Ph.D. dissertation*, Stanford Univ., Stanford, CA, 1981.
- [7] M. Varanasi, "Noncoherent detection in asynchronous multiuser channels," *IEEE Trans.*, Vol. IT-39, No. 1, 1993, pp. 157–176.
- [8] M. Varanasi and A. Russ, "Noncoherent decorrelative detection for nonorthogonal multipulse modulation over the multiuser Gaussian channel," *IEEE Trans.*, Vol. COM-46, No.12, 1998, pp. 1675–1684.
- [9] M. McCloud and L. Scharf, "Interference estimation with applications to blind multiple-access communication over fading channels," *IEEE Trans.*, Vol. IT-46, No. 5, 2000, pp. 947–961.
- [10] M. McCloud and L. Scharf, "Asymptotic analysis of the MMSE multiuser detector for nonorthogonal multipulse modulation," *IEEE Trans.*, Vol. COM-49, No. 1, 2001, pp. 24–30.
- [11] M. McCloud, L. Scharf, and M. Varanasi, "Beamforming, diversity, and interference rejection for multiuser communication over fading channels with a receive antenna array," *IEEE Trans.*, Vol. COM-51, No. 1, 2003, pp. 116–124.
- [12] A. Russ and M. Varanasi, "Noncoherent multiuser detection for nonlinear modulation over the Rayleigh fading channel," *IEEE Trans.*, Vol. IT-47, No. 1, 2001, pp. 295–307.
- [13] P. Stoica and R. Moses, *Introduction to Spectral Analysis*, Simon and Schuster, New York, 1997.
- [14] L. Scharf and B. Friedlander, "Matched subspace detectors", *IEEE Trans.*, Vol. SP-42, No. 8, 1994, pp. 2146–2157.
- [15] V. Tuzlukov, J.-H. Kim, and Y. D. Kim, "Performance comparison of FFH and MCFH spread spectrum wireless sensor network systems based on the generalized approach to signal processing", in *Proc. GSPx: The Embedded Signal Processing Conference*, September 27-30, Santa Clara, CA, USA, 2004.
- [16] M. Schwartzp, W. Bennett, and S. Stein, *Communication Systems and Techniques*, IEEE Press, New York, 1996.